JOURNAL OF ADVANCED TRANSPORTATION
J. Adv. Transp. 2013; **47**:43–60
Published online 10 September 2012 in Wiley Online Library (wileyonlinelibrary.com). **DOI**: 10.1002/atr.1205

Stepwise genetic fuzzy logic signal control under mixed traffic conditions

Yu-Chiun Chiou* and Yen-Fei Huang

Institute of Traffic and Transportation, National Chiao Tung University, 4F, 118 Sec. 1, Chung-Hsiao W. Rd. Taipei 10012, Taiwan

SUMMARY

This paper proposes a stepwise genetic fuzzy logic controller (SGFLC) by considering traffic flows and queue lengths of cars and motorcycles as state variables and extension of green time as control variable, towards the minimization of total vehicle delays. For the learning efficiency of SGFLC and the capability in capturing traffic behaviors of Asian urban streets, where mixed traffic of cars and motorcycles are prevailing, the mixed traffic cell transmission model (MCTM) is introduced to replicate traffic behaviors. To investigate the control performance of the proposed SGFLC model, comparisons with two pre-timed timing plans and three adaptive signal timing models are conducted at an isolated intersection. Results show our proposed SGFLC model performs best. Moreover, as traffic flows vary more noticeably, the SGFLC model performs even better. In the experimental and field cases of three-intersection arterial under four coordinated signal systems, namely simultaneous, progressive, alternate and independent, both cases consistently show that the proposed SGFLC model perform best, suggesting that the proposed SGFLC signal control model is efficient and robust.

KEY WORDS: adaptive signal control; genetic fuzzy logic controller; stepwise learning algorithm; mixed cell transmission model

1. INTRODUCTION

Adaptive traffic signal control typically feeds the real-time traffic data, collected by the sensors, into a built-in controller to produce the timing plans. Thus, it can provide signal-timing plans in response to real-time traffic conditions. Actuated signal control, dynamic signal control, and adaptive signal control are examples of on-line control. Because of its flexibility, applicability and optimality, adaptive signal control tends to be the mainstream of signal controls nowadays. The well-known adaptive signal controllers, such as SCOOT, SCATS, and OPAC, employ mathematical equations or models to determine "crisp" threshold values as the cores of control mechanism; thus, the control performance could be negatively affected by the uncertainty of traffic conditions. Because a fuzzy control system has excellent performance in data mapping as well as in treating ambiguous or vague judgment [1], many recent works have employed fuzzy set theory to develop fuzzy logic controllers (FLC), also known as fuzzy control system, fuzzy inference system, approximate reasoning, or expert system. The applications of FLC to signal control are to determine the signal phasing and timing plans, including priority of phases, cycle length and split, by utilizing the real-time traffic data, such as vehicle arrival or arrival rate, occupancy, queue length and speed, collected by detectors.

*Correspondence to: Yu-Chiun Chiou, Institute of Traffic and Transportation, National Chiao Tung University, 4F, 118 Sec. 1, Chung-Hsiao W. Rd., Taipei 10012, Taiwan. E-mail: ycchiou@mail.nctu.edu.tw

In FLC systems, both inference engine and defuzzification have been consistently used in previous literature; however, methods for formulating the rule base (logic rules) and data base (membership functions) are subjectively preset, not optimally solved. Adjusting the combination of logic rules and membership functions very often requires tremendous efforts, but there is no guarantee to obtain good control performance. Genetic algorithms (GAs) have been proven suitable for solving both combinatory optimization problem (e.g., selecting the logic rules) and parameter optimization problem (e.g., tuning the membership functions). Employing GAs to construct an FLC system with learning process from examples, hereafter termed as genetic fuzzy logic controller (GFLC), can not only avoid the bias caused by subjective settings of logic rules or membership functions but also greatly enhance the control performance.

Most previous GFLC studies, however, have employed GAs either to calibrate the membership functions with preset logic rules or to select the logic rules with given membership functions. Thus, the applicability of that GFLC is very likely reduced. However, to simultaneously or sequentially learn of logic rules and membership, functions may require a rather lengthy chromosome and large search space, resulting into poor performance, a long convergence time and unreasonable learning results (i.e., conflicting or redundant logic rules and irrational shapes of membership functions). To avoid these shortcomings, this paper proposes a stepwise evolution algorithm to learn both logic rules and membership functions. At each learning process, the proposed algorithm selects one logic rule, which can best contribute to the overall performance controlled by previously selected logic rules combined with this selected rule. Such a selection procedure will be repeated until no other rule can ever improve the control performance. Therefore, the incumbent combination of logic rules is the optimal learning results.

However, to develop a stepwise genetic fuzzy logic controller (SGFLC)-based signal control requires an efficient traffic simulation model to replicate traffic behaviors and determine the performance of the control logic. Although many studies use an application programming interface via microscopic traffic simulation software to simulate the urban signal control and implement the optimized signal policy, such as AIMSUN [2,3], PARAMICS [4–6], VISSIM [7–9] and CORSIM [10,11]. However, such simulation software would be rather time consuming, making it better for evaluating the control performance for a given signal control model, but not suitable for the evolution of genetic generations for model training. Thus, this paper employs a cell transmission model (CTM), proposed by Daganzo [12,13], to evaluate the performance of learned logic rules and tuned membership function. Besides, the conventional CTM was designed for pure traffic. Incorporation of more realistic CTM rules into the simulation of mixed traffic (various types of vehicles such as cars and motorcycles) on urban streets is comparatively less addressed. On this basis, this study conducted mixed traffic cell transmission models (MCTM), proposed by Chiou and Hsieh [14], to replicate the behaviors of mixed traffic consisting of cars and motorcycles. The MCTM model uses the ratio of car to motorcycle in the last upstream cell to determine the amount of roadway resources (i.e., max flow capacity and storage capacity) allocated to cars, and vice versa for motorcycles. In order to describe the relationship between cars and motorcycles more realistically, the MCTM model further incorporates an entropy index to adjust the traffic speed, because the interferences between two types of vehicles will be rapidly increased as the mixture ratio of cars and motorcycles becomes higher.

On this basis, this paper aims to develop an adaptive signal control model for both isolated and sequential intersections based on the proposed SGFLC with an MCTM approach. The paper is organized as follows. Section 2 briefs the rationales for signal control with SGFLC and MCTM models. Section 3 presents the validation of the MCTM model in replicating real traffic hydrodynamic behaviors. Section 4 utilizes experimental cases to validate the effectiveness and robustness of the proposed SGFLC model in controlling the signal at an isolated intersection. Section 5 further validates the effectiveness of the SGFLC model in controlling the signal of arterial coordinated sequential intersections. Finally, the concluding remarks and suggestions for future research follow.

DOI: 10.1002/atr

2. THE RATIONALES

2.1. The stepwise genetic fuzzy logic controller model

The encoding methods, genetic operators and stepwise evolution algorithm for the SGFLC model are briefly described as follows.

2.1.1. Encoding logic rules and membership functions

Consider a triangle fuzzy number and let parameters c^{r}, c^{c} and c^{l} respectively represent the coordinates of right anchor, cortex and left anchor of a linguistic degree as shown in Figure 1. Therefore, a variable with a linguistic degree has three parameters that need to be calibrated in the following order:

$$c^{\mathrm{l}} \leq c^{\mathrm{c}} \leq c^{\mathrm{r}} \tag{1}$$

To avoid the violation of the aforementioned order of these three parameters, three 3-position variables r_1–r_3 are designed as follows:

$$c^{\mathrm{l}} = r_1 \tag{2}$$

$$c^{\mathrm{c}} = r_1 + r_2 \tag{3}$$

$$c^{\mathrm{r}} = r_1 + r_2 + r_3 \tag{4}$$

To achieve two significant digits, each position variable is represented by four real-coding genes also depicted in Figure 1. The maximum value of the position variables is 99.99 and the minimum value is 0. Thus, in the example of two state variables and one control variable, the chromosome is composed of 36 genes.

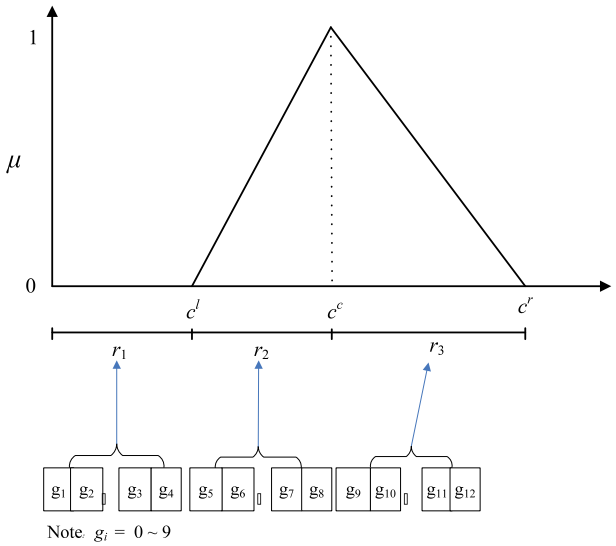

Figure 1. Encoding method for logic rules and membership functions.

DOI: 10.1002/atr

2.1.2. Genetic operations

The max-min-arithmetical crossover and the non-uniform mutation are adopted. In the max-min-arithmetical crossover, let $G_w^t = \{g_{w1}^t, \ldots, g_{wk}^t, \ldots, g_{wK}^t\}$ and $G_v^t = \{g_{v1}^t, \ldots, g_{vk}^t, \ldots, g_{vK}^t\}$ be two chromosomes selected for crossover, the following four offsprings will be generated [15]:

$$G_1^{t+1} = aG_w^t + (1-a)G_v \tag{5}$$

$$G_2^{t+1} = aG_v^t + (1-a)G_w^t \tag{6}$$

$$G_3^{t+1} \text{with } g_{3k}^{t+1} = \min\{g_{wk}^t, g_{vk}^t\} \tag{7}$$

$$G_4^{t+1} \text{with } g_{4k}^{t+1} = \max\{g_{wk}^t, g_{vk}^t\} \tag{8}$$

where a is a parameter ($0 < a < 1$) and t is the number of generations. In the non-uniform mutation, let $G_t = \{ g_1^t, \ldots, g_k^t, \ldots, g_K^t \}$ be a chromosome and the gene g_k^t be selected for mutation (the domain of g_k^t is $[g_k^l, g_k^u]$), the value of g_k^{t+1} after mutation can be computed as follows [16]:

$$g_k^{t+1} = \begin{cases} g_k^t + \Delta\left(t, g_k^u - g_k^t\right) & \text{if} \quad b = 0 \\ g_k^t - \Delta\left(t, g_k^t - g_k^l\right) & \text{if} \quad b = 1 \end{cases} \tag{9}$$

where b randomly takes a binary value of 0 or 1. The function $\Delta(t, z)$ returns a value in the range of [0, z] such that the probability of $\Delta(t, z)$ approaches to 0 as t increases:

$$\Delta(t, z) = z\left(1 - r^{(1-t/T)^h}\right) \tag{10}$$

where r is a random number in the interval [0,1], T is the maximum number of generations and h is a given constant. In Equation (10), the value returned by $\Delta(t, z)$ will gradually decrease as the evolution progresses.

2.1.3. The stepwise learning algorithm

The core logic of the proposed stepwise algorithm in selecting the logic rules with the membership functions is similar to the stepwise regression model in selecting explanatory variables. At each stage, a new logic rule that can best increase the control performance by combining with the rules chosen in previous stages is selected. The selection process continues until the control performance cannot be improved by introducing any other rule. The stepwise learning algorithm is structured as follows:

Step 0 Initialization: $s = 1$. The rule combination set, SR_s, is an empty set.
Step 1 Update rule combination set. $SR_s = SR_{s-1} + R_s$.
Step 2 Tuning membership functions.
Step 2-1 Generating an initial population with p chromosomes. Each chromosome representing a logic rule has $12(n+1)$ genes, and each gene randomly takes one integer from $[0, 9]$. n is the number of state variables.
Step 2-2 Calculating the fitness values of all chromosomes based on the logic rule represented by the chromosome and previously selected logic rules.
Step 2-3 Selection.
Step 2-4 Crossover.
Step 2-5 Mutation.
Step 2-6 Testing the stop condition. Let R_s be the chromosome with largest fitness of f_s among the population for the *sth* evolution epoch. The stop condition is set on the basis of whether the mature rate has reached a given constant η. If so, proceed to Step 3 and let $s = s + 1$; otherwise, go to Step 2-3.
Step 3 Testing the stop condition. If $(f_s - f_{s-1}) \leq \varepsilon$, where ε is an arbitrary small number, then stops. Incumbent rule combination set, SR_s, is the optimal learning result. Otherwise, go to Step 1.

DOI: 10.1002/atr

2.2. The signal control

2.2.1. Fitness value

The performances of signal control for an isolated intersection or sequential intersections are commonly measured in terms of total number of stopped vehicles, proportion of stopped vehicles, average vehicle delays, total vehicle delays, maximal green band, and so on. This paper sets the total vehicle delays (TVD) as the control performance index and thus defines the fitness function of GAs as

$$f = \frac{1}{TVD} \tag{11}$$

2.2.2. State variables

Following most of the previous literature, for the case of an isolated intersection, we choose traffic flow in green phase (*TF*) and queue length in red phase (*QL*) as two state variables and extension of green time (*EGT*) as the control variable. For the case of sequential intersections, *TF* is the summation of traffic flows at all approaches in green phase; whereas *QL* is the summation of queen length at all approaches in red phase.

To reflect the different details of mixed traffic flow, three models with different considerations of state variables are developed. Model 1 considers four state variables: traffic flow of cars (*TFC*), traffic flow of motorcycles (*TFM*), queue length of cars (*QLC*) and queue length of motorcycles (*QLM*). Model 2 considers two state variables by weighted summing up cars and motorcycle traffic: traffic flow *TFP* ($TFP = TFC + \alpha TFM$) and queue length *QLP* ($QLP = QLC + \alpha QLM$), where α is the passenger car equivalent (PCE) of motorcycles (0.3 in this study). Model 3 also considers two state variables by simply summing up car and motorcycle traffic: traffic flow *TFV* ($TFV = TFC + TFM$) and queue length *QLV* ($QLV = QLC + QLM$).

2.2.3. Activation points

In consideration of pedestrian safe crossing, a minimum green time ($G_{\min}$) in each green phase is preset both for an isolated intersection or sequential intersections. At the end of $G_{\min}$, the proposed SGFLC model is activated automatically to conclude an *EGT*. If $EGT \geq EGT_{\min}$ (a preset value), current green phase is extended by *EGT* seconds. If $EGT < EGT_{\min}$, current green phase is then terminated. The SGFLC model will not be activated again until the end of this extension time. If total green time exceeds the preset maximum green time ($G_{\max}$), current green phase is forced to terminate. A short all-red (*AR*) period is designed in each signal change interval. The activation points for an isolated intersection are also depicted in Figure 2(a).

This paper also uses the SGFLC model to adaptively control the signals of sequential intersections along an arterial. To reflect the various traffic conditions of different coordinated intersections, the green times along the arterial are independently determined by following the same control mechanism of an isolated intersection. However, to synchronize the signal timing plans of all coordinated intersections, an integrated signal control mechanism is activated by considering the summation of traffic flows at all approaches in green phase and summation of queen length at all approaches in red phase. Therefore, the cycle length of all coordinated intersections is kept the same. It should be noted that the activation of extended red time of the arterial (i.e., the extended green time of competing approaches) will not be started until all intersections along the arterial have been turned into red phase. Figure 2(b) illustrates the activation points and signal timings for one of the sequential intersections.

3. MIXED-TRAFFIC CELL TRANMISSIONS MODEL

The core logic and validation results of the MCTM are briefly narrated as follows.

3.1. The mixed traffic cell-transmission model

To facilitate the learning process of the proposed SGFLC model, an efficient traffic simulator is imperative to evaluate the performance of selected logic rules and tuned membership functions in a short

DOI: 10.1002/atr

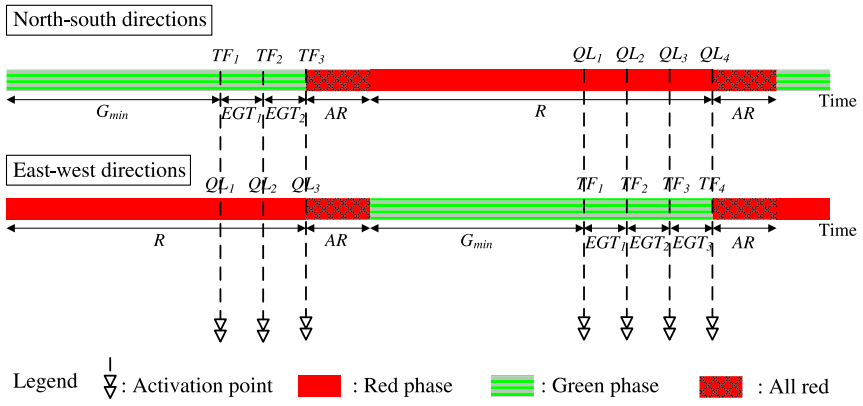

(a) Isolated intersection

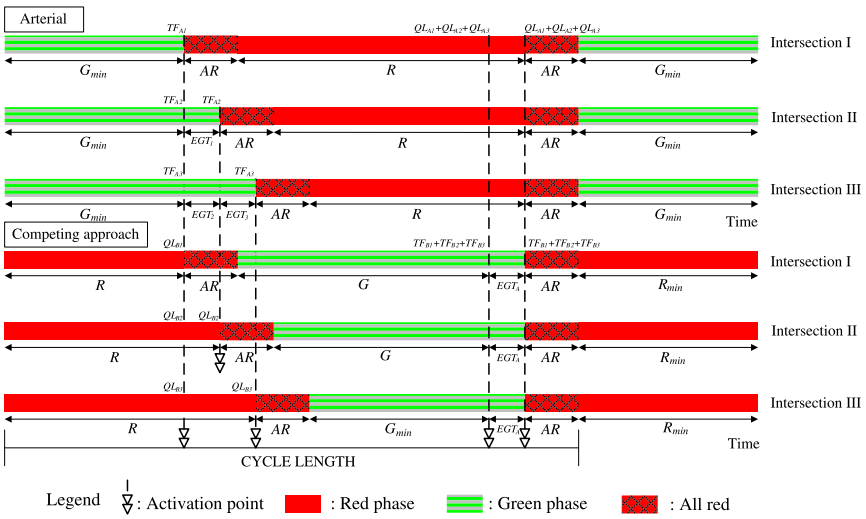

(b) Sequential intersection

Figure 2. Activation points for an (a) isolated intersection and (b) sequential intersections.

period. On this basis, a cell-based traffic simulator CTM is considered. CTM, proposed by Daganzo [12,13] for simulating traffic hydrodynamic behavior, uses several simple equations to govern traffic movements along the roadway, which is represented by a series of equal-length cells. These equations are expressed as follows:

$$n_i(t+1) = n_i(t) + y_i(t) - y_{i+1}(t) \tag{12}$$

$$y_i(t) = \min\{n_{i-1}(t), q_{\mathrm{mi}}(t), \beta[N_i(t) - n_i(t)]\} \tag{13}$$

$$\beta = \begin{cases} 1, & \text{if } n_{i-1}(t) \le q_{\mathrm{mi}}(t) \\ \dfrac{w}{v}, & \text{if } n_{i-1}(t) \ge q_{\mathrm{mi}}(t) \end{cases} \tag{14}$$

On the basis of the pure traffic CTM, Chiou and Hsieh [14] developed and validated an MCTM for the traffic flow of cars and motorcycles. In Chiou and Hsieh's model, the variable $n_i(t)$ is decomposed into $n_i^c(t)$ and $n_i^m(t)$ for representing the numbers of cars and motorcycles in cell i at time t, respectively. Thus, Equation (12) can be revised as follows:

DOI: 10.1002/atr

$$\begin{aligned} n_i^c(t+1) &= n_i^c(t) + y_i^c(t) - y_{i+1}^c(t) \\ n_i^m(t+1) &= n_i^m(t) + y_i^m(t) - y_{i+1}^m(t) \end{aligned} \tag{15}$$

Both types of vehicles exhibit rather different traffic behaviors in competing for roadway capacity and remaining storage space. Thus, the parameters of the MCTM, including maximal flow rate, maximal storage capacity, and remaining storage capacity, should be dynamically adjusted and allocated between cars and motorcycles according to mixture ratio of vehicles types. Depending upon various traffic conditions, three situations are detailed as follows:

(1) Free-flow condition: no competition between cars and motorcycles

The flow and density of cars and motorcycles, in the upstream cell, are less than the maximal flow and remaining capacity in the downstream cell. This condition refers to the first condition of Equation (13), which the vehicles can transmit from upstream to downstream without any deterrent.

(2) Maximal flow ($q_{mi}(t)$) competition between cars and motorcycles

This situation occurs when the number of cars and motorcycles in the upstream cell exceeds maximal flow (i.e., the second condition of Equation (13)). Thus, cars and motorcycles compete to transmit from upstream cell to downstream cell. This competition behavior can be elaborated as follows:

$$\begin{aligned} Q_i^m(t) &= \frac{\left[R_m^Q\left(n_{i-1}^c(t), n_{i-1}^m(t)\right) \times q_{\mathrm{mi}}(t)\right]}{\alpha} \\ Q_i^c(t) &= \left[1 - R_m^Q\left(n_{i-1}^c(t), n_{i-1}^m(t)\right)\right] \times q_{\mathrm{mi}}(t) \end{aligned} \tag{16}$$

where flow competition functions $R^Q\left(n_{i-1}^c(t), n_{i-1}^m(t)\right)$, is a function of the number of cars and motorcycles.

According to our field observations, the interferences between cars and motorcycles are rapidly increased as the mixture ratio of cars and motorcycles becomes higher. Thus, Chiou and Hsieh [14] introduced the entropy concept to dynamically adjust PCE by defining the competition relationship as

$$R_m^Q\left(n_{i-1}^c(t), n_{i-1}^m(t)\right) = \frac{\eta \times n_{i-1}^m(t)}{\eta \times n_{i-1}^m(t) + n_{i-1}^c(t)} \tag{17}$$

where η is the adjusted PCE of motorcycles, which is assumed to linearly increase as the entropy can become higher from a base value of PCE (α):

$$\eta = \alpha + (\varepsilon \times H(n_{i-1}(t))) \tag{18}$$

where $H(n_{i-1}(t))$ is an entropy function measured by the proportions of cars (p^c) and motorcycles (p^m):

$$H(n_{i-1}(t)) = -\left[p^m(n_{i-1}(t)) \log p^m(n_{i-1}(t)) + p^c(n_{i-1}(t)) \log p^c(n_{i-1}(t))\right] \tag{19}$$

The proportions of cars (p^c) and motorcycles (p^m) in upstream cell can be calculated by Equations (20) and (21), respectively:

$$p^c(n_{i-1}(t)) = \frac{l \times n_{i-1}^c(t)}{n_{i-1}^m(t) + l \times n_{i-1}^c(t)} \tag{20}$$

$$p^m(n_{i-1}(t)) = \frac{n_{i-1}^m(t)}{n_{i-1}^m(t) + l \times n_{i-1}^c(t)} \tag{21}$$

where, l is the space of a car/motorcycle.

DOI: 10.1002/atr

(2) Remaining storage capacity ($N_i(t) - n_i(t)$) competition between cars and motorcycles

This competition behavior occurs when remaining storage capacity in the downstream cell cannot accommodate all vehicles transmitting from the upstream cell (i.e., $l \times n_{i-1}^c(t) + n_{i-1}^m \geq S_i(t)$). In addition, the motorcycles can still "sneak" into the downstream cell when remaining storage capacity cannot accommodate a car. To reflect on this phenomenon, a congestion index (δ) is introduced to determine how the remaining storage space ($S_i(t)$) is allocated:

$$S_i(t) = \delta \times \left\{ N_i(t) i - \left[l \times n_i^c(t) + n_i^m(t) \right] \right\} \tag{22}$$

where

$$\delta = \begin{cases} 1 & \text{if } n_{i-1}^c(t) + \alpha \times n_{i-1}^m(t) \leq q_{\mathrm{mi}}(t) \\ \dfrac{w}{v} & \text{if } n_{i-1}^c(t) + \alpha \times n_{i-1}^m(t) > q_{\mathrm{mi}}(t) \end{cases}$$

Consider a space competition function, $R_m^S\left(n_{i-1}^c(t), n_{i-1}^m(t)\right)$, which allocates remaining storage space between cars and motorcycles moving from upstream to downstream. The remaining storage capacity is then allocated to cars $\left(S_i^c(t)\right)$ and motorcycles $\left(S_i^m(t)\right)$ and is expressed as follows:

$$S_i^c(t) = R_m^S\left(n_{i-1}^c(t), n_{i-1}^m(t)\right) \times S_i(t) \tag{23}$$

$$S_i^m(t) = \frac{\left[1 - R_m^S\left(n_{i-1}^c(t), n_{i-1}^m(t)\right)\right] \times S_i(t)}{l} \tag{24}$$

Logghe and Immers [17] indicated that higher density of vehicles of class i on the road has the advantage to move forward. Thus, the competition functions can be expressed as

$$R_m^S\left(n_{i-1}^c(t), n_{i-1}^m(t)\right) = \frac{n_{i-1}^m(t)}{n_{i-1}^m + l \times n_{i-1}^c(t)} \tag{25}$$

In sum, with the pure traffic CTM proposed by Daganzo in Equations (12) and (13), the mixed traffic CTM with cars and motorcycles proposed by Chiou and Hsieh [14] can replicate mixed traffic with Equations (26) and (27).

$$\begin{aligned} n_i^c(t+1) &= n_i^c(t) + y_i^c(t) - y_{i+1}^c(t) \\ n_i^m(t+1) &= n_i^m(t) + y_i^m(t) - y_{i+1}^m(t) \end{aligned} \tag{26}$$

$$\begin{aligned} y_i^c(t) &= \min\left\{ n_{i-1}^c(t), \left[1 - R_m^Q\left(n_{i-1}^c(t), n_{i-1}^m(t)\right)\right] \times q_{mi}(t), \frac{\left[1 - R_m^S\left(n_{i-1}^c(t), n_{i-1}^m(t)\right)\right] \times S_i(t)}{l} \right\} \\ y_i^m(t) &= \min\left\{ n_{i-1}^m(t), \frac{\left[R_m^Q\left(n_{i-1}^c(t), n_{i-1}^m(t)\right) \times q_{mi}(t)\right]}{\alpha}, R_m^S\left(n_{i-1}^c(t), n_{i-1}^m(t)\right) \times S_i(t) \right\} \end{aligned} \tag{27}$$

3.2. Validation

To validate the MCTM in replicating the traffic behaviors at signalized intersections in Taiwan, field traffic data were collected at one of the approaches of a signalized intersection in Taipei on 27 February 2009. The study approach was divided into six cells depending on free-flow speed and length of time step, as shown in Figure 3. The traffic moves from cell 1 to cell 6 and y_I and y_O denote the traffic flows in and out the study approach, respectively. The stop line of the intersection is located at the right bound of cell 6.

DOI: 10.1002/atr

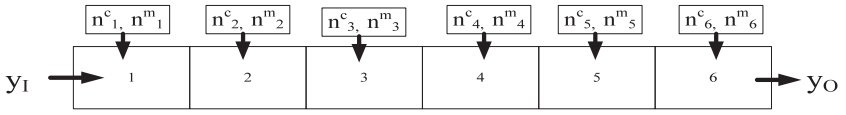

Figure 3. Configuration of the validated approach.

The performance of the MCTM model is shown in Table 1. As noted from Table 1, the MAPE values are less than 30% in most of the cells in both green and red time. In addition, the simulation results are more accurate at the cells closer to the stop line and for motorcycle traffic.

According to the number of vehicles and flow at cell 6 in red time and green time, this study also validates the queuing behavior in red phase and platoon dispersion in green phase. The results are shown in Figure 4(a) and (b), respectively. The results show that the proposed mixed CTM can satisfactorily replicate the traffic behaviors at the signalized intersection.

4. EXPERIMENTAL EXAMPLE: ISOLATED INTERSECTION

To investigate the effectiveness and robustness of the proposed signal control model, comparisons to two pre-timed models and three adaptive models are conducted at an experimental isolated intersection.

4.1. Model training

To validate the effectiveness and robustness of the proposed SGFLC signal control model, an experimental example for an isolated four-leg intersection (Figure 5) is demonstrated. To simplify the analysis, the turning traffic is neglected. The parameters of the MCTM model are set as: free-flow speed = 50 km/hour, time step = 2 seconds, $k_j = 130$ veh/km/lane. Assume that the intersection has two lanes ($N_i(t) = 3.6$ cars/cell for all i and t) in each approach with saturation flow of 1800 pcu/hour/lane ($q_{\mathrm{mi}}(t) = 2.00$ veh/time step for all i and t). The flow patterns of 5-minute flow rates in different

Table I. Validation results of the mixed traffic cell-transmission model in different cells and phases.

			Cell						
Phase	Performance	Vehicle types	1	2	3	4	5	6	y_{6I}
Green (120 seconds)	MAPE	Car (%)	26.71	42.80	34.46	10.90	16.81	15.79	8.05
		Motorcycle (%)	23.60	38.95	30.63	3.38	8.17	11.75	3.48
	RMSE	Car	17.70	20.75	19.01	10.17	13.17	21.09	5.16
		Motorcycle	24.85	32.56	26.06	4.50	11.29	25.59	6.05
Red (50 seconds)	MAPE	Car (%)	30.42	11.42	24.60	28.24	27.66	11.49	—
		Motorcycle (%)	6.21	26.89	27.40	21.19	33.31	16.21	—
	RMSE	Car	2.03	0.71	3.18	22.06	32.33	31.56	—
		Motorcycle	1.12	3.30	3.84	6.98	13.96	91.87	—

MAPE, mean absolute percentage error; RMSE, root-mean-square error.

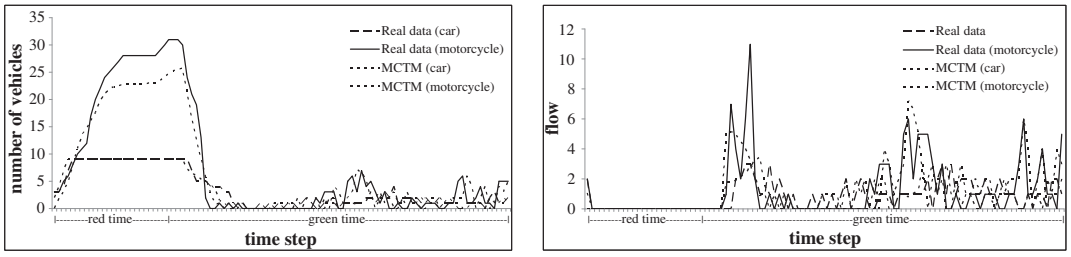

(a) Number of vehicles (b) Flow

Figure 4. (a) Number of vehicles and (b) flow at cell 6 in red time and green time.

DOI: 10.1002/atr

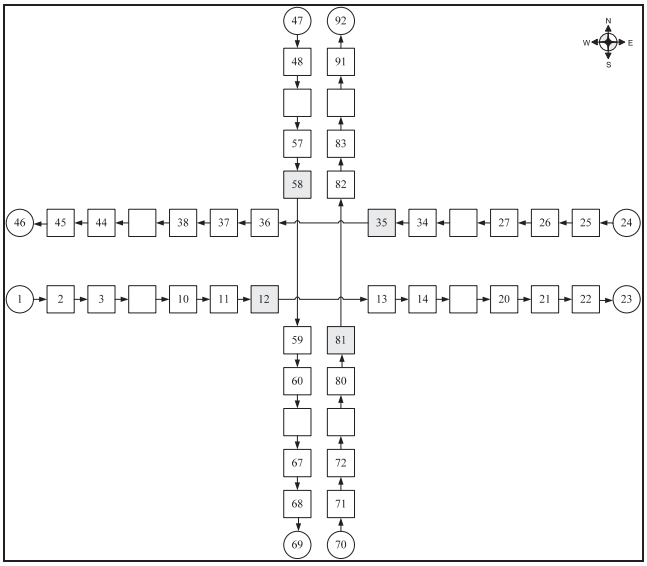

Figure 5. Configuration of the experimental isolated intersection.

approaches are given in Figure 6. A noticeable peak and off-peak traffic patterns are assumed in east and west directions; whereas rather flat traffic patterns are assumed in north and south directions. The parameters of the SGFLC model are set the same as those in Chiou and Lan [18]. The center of gravity method is employed for defuzzification. The parameters of signal control are: $G_{\max} = 100$ seconds, $G_{\min} = 20$ seconds, all red + lost time = 6 seconds, $EGT_{\max} = 20$ seconds, and $EGT_{\min} = 4$ seconds.

4.2. *Model performance*

Table 2 compares the control performances of three SGFLC models. As shown in Table 2, Model 1 performs best with lowest *TVD* of 46.67 vehicle-hour, suggesting that the more details in traffic measurement, the better performance can be achieved. In what follows, only the learning results and control performance of Model 1 is further elaborated and compared.

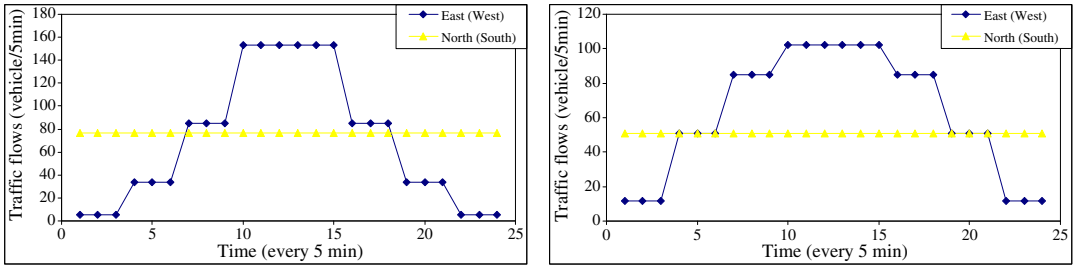

(a) car flow rates (b) motorcycle flow rates

Figure 6. Five-minute (a) car and (b) motorcycle flow rates at the experimental isolated intersection.

Table II. Control performances of the SGFLC models with various state variables.

Models	State variables	Generations	*TVD*	Number of selected rules
Model 1	*TFC,TFM,QLC* and *QLM*	60	46.67	5
Model 2	*TFP* and *QLP*	76	52.02	8
Model 3	*TFV* and *QLV*	90	52.15	7

SGFLC, stepwise genetic fuzzy logic controller; TVD, total vehicle delays; TFC, traffic flow of cars; TFM, traffic flow of motorcycles; QLC, queue length of cars; QLM, queue length of motorcycles; TFP = $(TFC + \alpha TFM)$; QLP = $(QLC + \alpha QLM)$; $TFV = (TFC + TFM)$; $QLV = (QLC + QLM)$; α = PCE, passenger car equivalent.

DOI: 10.1002/atr

The learning process of Model 1 is depicted in Figure 7(a). Note that SGFLC converges after five stepwise evolutions with a total of 60 generations progressed. The value of *TVD* decreases from 66.47 to 46.67 vehicle-hour. A total of five rules are selected after five stepwise evolutions. Figure 7(b) presents the optimally selected five logic rules along with corresponding tuned membership functions.

4.3. Model validation and comparisons

To validate the effectiveness, the control performance of the SGFLC model is compared with two pre-timed models: optimal single (OS) and optimal multiple (OM) and three adaptive models: iterative genetic fuzzy logic control (IGFLC) model, vanishing queue (VQ) and maximum queue (MQ), where the OS timing plan is determined by total enumeration method to search for an optimal cycle length and green time during the study period. The OM timing plan, comprising seven optimal single timing plans, depends on traffic flow pattern as shown in Figure 4. Because the OM model designs the optimal signal timings for each of traffic flow rates, its control performance is optimal for the given traffic pattern. The IGFLC model proposed by Chiou and Lan [18] is to simultaneously and iteratively select all combination rules and then tune all membership functions of linguistic variables. The VQ model proposed by Lin and Lo [19] is an actuated control system that switches traffic signal to serve the other approach whenever the queue on the current approach vanishes; whereas the MQ model switches traffic signal to serve the other approach when the queue length on the that approach reaches a preset maximum queue. In this paper, the maximum queue length is optimized via a trial-and-error manner.

Table 3 summarizes the comparison results. Comparing to the OS model, the proposed SGFLC model can curtail 4.36 vehicle-hours (8.54%) and incur only 0.66 more vehicle-hours (1.43%) delays

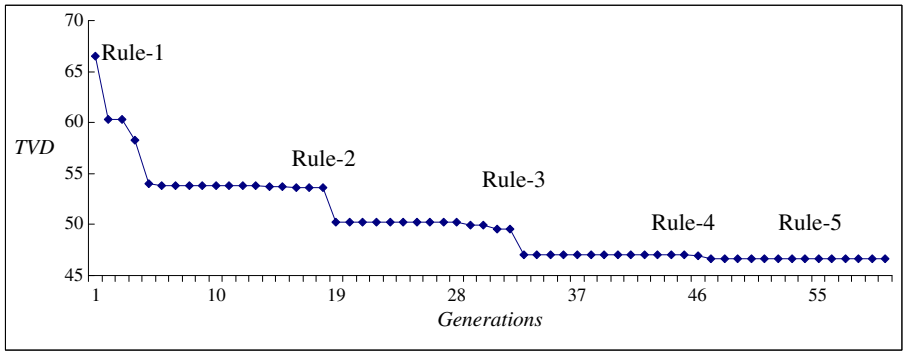

(a) Learning process

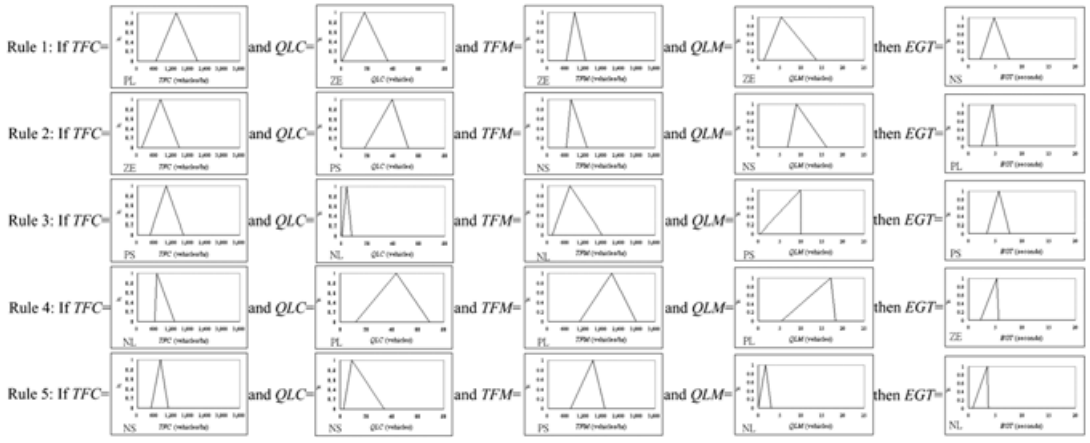

(b) Selected logic rules and tuned membership functions

Figure 7. (a) Learning process and (b) selected logic rules and tuned membership function results of the stepwise genetic fuzzy logic controller model at the experimental intersection.

DOI: 10.1002/atr

than the OM model, suggesting the proposed SGFLC model almost can achieve the optimal control. Comparing to three adaptive models, the SGFLC model performs better than the IGFLC, VQ and MQ models by respectively curtailing 0.06, 2.22 and 4.59 vehicle-hours (0.13%, 4.54% and 8.95%) of total vehicle delays, demonstrating the effectiveness of our proposed SGFLC model.

Moreover, according to the learning results of two similar GFLC models, the SGFLC and IGFLC, as shown in Table 4, although both GFLC models exhibit high control performance, the proposed SGFLC model selects much fewer rules (only five rules) with a fewer generation than the IGFLC model does (401 rules). Additionally, by examining the rules selected by the IGFLC model, many of them are redundant or mutually conflicting. The merit of selecting few rules provides a chance for post-optimization adjustment and rule interpretation. Thus, the comparison shows that the proposed SGFLC is more effective, efficient and comprehensible than the IGFLC model.

The green splits determined by the SGFLC model are depicted in Figure 8(b), which are in coincidence with the traffic patterns in Figure 8(a), suggesting that the proposed SGFLC can control the signal responsively. Figure 8(c) further presents the average delays of cars and motorcycles. As the traffic grows, the average delays of both cars and motorcycles are significantly increased. It is interesting to note that the average delay of cars grow much more rapidly than that of motorcycles because motorcyclists do not follow the lane disciplines. They may make lateral drifts breaking into two moving cars. Once blocked by the front vehicles, they even make wide transverse crossings through the gap between two stationary cars in the same lane, in order to keep moving forward. The behaviors are in accordance with our field observations and the cellular automaton model proposed by Lan *et al*. [20].

To further examine the robustness of the SGFLC model, we randomly vary the traffic flows by 10–50% as shown in Figure 9. Assume that timing plans of pre-timed models (i.e., the OS and OM) remain unchanged and the adaptive models follow the same rules learned from the original traffic patterns given in Figure 4. The results are summarized in Table 5. Note that the SGFLC model performs best among the pre-timed and adaptive models. Moreover, the SGFLC model can do much better than any other models as the traffic flows vary more conspicuously, indicating the robustness of the SGFLC model.

5. EXPERIMENTAL EXAMPLE: SEQUENTIAL INTERSECTIONS

This paper further extends the proposed SGFLC model to the signal control of consecutive intersections. These sequential intersections contain an arterial (east–west direction) and three competing approaches (north–south direction). To synchronize the signal control for the sequential intersections,

Table III. Comparisons of control models at the experimental isolated intersection.

		ΔTVD compared with SGFLC	
Models	*TVD* (vehicle-hours)	(vehicle-hours)	(%)
SGFLC	46.67	—	—
OS	51.03	4.36	8.54
OM	46.01	−0.66	−1.43
IGFLC	46.73	0.06	0.13
VQ	48.89	2.22	4.54
MQ	51.26	4.59	8.95

TVD, total vehicle delays; SGFLC, stepwise genetic fuzzy logic control; OS, optimal single; OM, optimal multiple; IGFLC, iterative genetic fuzzy logic control; VQ, vanishing queue; MQ, maximum queue.

Table IV. Learning results of the SGFLC and IGFLC models.

Models	State variables	Generations	*TVD*	Number of selected rules
SGFLC	*TFC,TFM,QLC* and *QLM*	60	46.67	5
IGFLC	*TFC,TFM,QLC* and *QLM*	314	46.73	401

SGFLC, stepwise genetic fuzzy logic control; IGFLC, iterative genetic fuzzy logic control; TFC, traffic flow of cars; TFM, traffic flow of motorcycles; QLC, queue length of cars; QLM, queue length of motorcycles.

DOI: 10.1002/atr

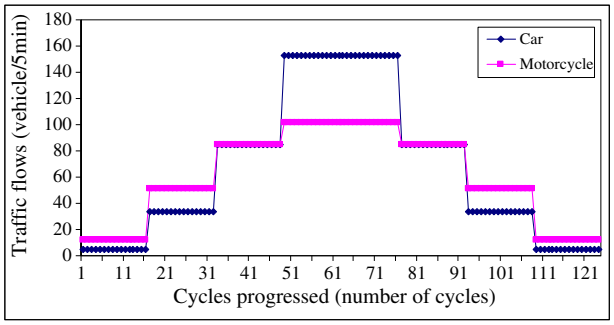

(a) Traffic flow rates of cars and motorcycles

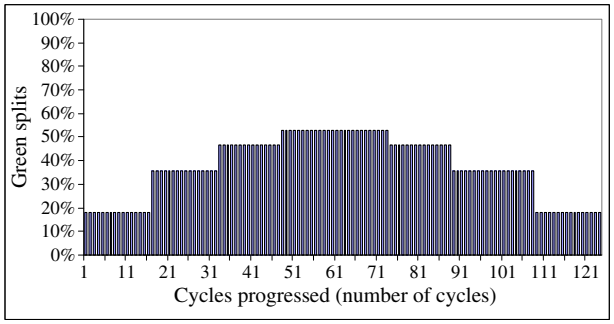

(b) Green splits

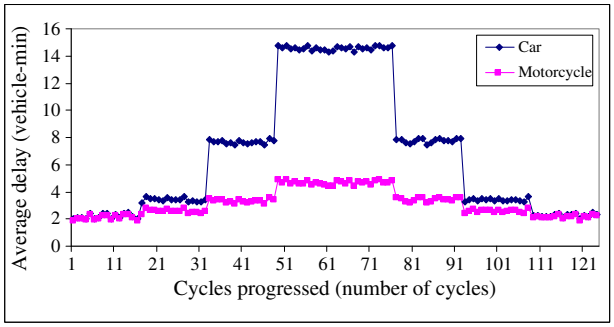

(c) Average delays of cars and motorcycles

Figure 8. (a) Traffic flow rates, (b) green splits and (c) average delay of east–west traffic.

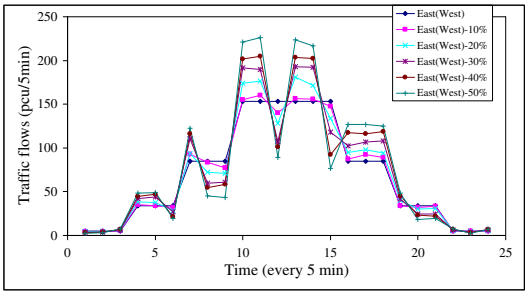

(a) car flow charts

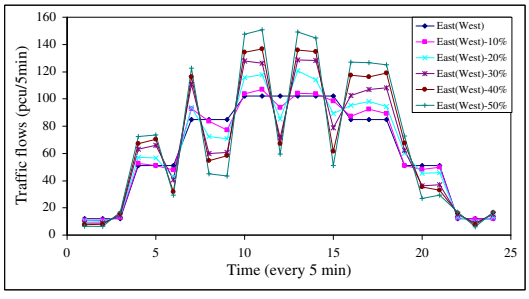

(b) motorcycle flow charts

Figure 9. Varied five-minute (a) car and (b) motorcycle flow rates at the experimental isolated intersection.

three coordinated signal systems including simultaneous, alternate, and progressive systems are considered. The simultaneous system implements exactly the same signal timing plans simultaneously in sequential intersections without offset (time lag). The progressive system implements these plans

DOI: 10.1002/atr

Table V. Comparisons of control performance with randomly varied flow rates.

	10%		20%		30%		40%		50%	
Models	*TVD*	Δ*TVD* (%)	*TVD*	Δ*TVD* (%)	*TVD*	Δ*TVD* (%)	*TVD*	Δ*TVD* (%)	*TVD*	Δ*TVD* (%)
SGFLC	48.74	—	48.81	—	52.01	—	53.24	—	55.13	—
OS	55.41	13.68	61.45	25.90	66.57	27.99	70.12	31.71	74.98	36.01
OM	52.02	6.73	52.88	8.34	56.81	9.23	60.47	13.58	65.54	18.88
IGFLC	50.40	3.41	53.52	9.65	57.32	10.21	58.83	10.50	61.04	10.72
VQ	50.04	2.67	51.91	6.35	55.46	6.63	57.00	7.06	59.64	8.18
MQ	52.47	7.65	53.14	8.87	56.97	9.54	61.16	14.88	65.77	19.30

TVD, total vehicle delays; SGFLC, stepwise genetic fuzzy logic control; OS, optimal single; OM, optimal multiple; IGFLC, iterative genetic fuzzy logic control; VQ, vanishing queue; MQ, maximum queue.

with offset. The alternative system implements two timing plans with inverse green and red times. In addition, an independent operation that implements the timing plans at the sequential intersections without any coordination is also compared. The timing plans of these four signal systems are determined by the SGFLC, IGFLC, VQ and MQ models, respectively.

5.1. Model training

The difference of signal control between an isolated intersection and coordinated sequential intersections is that the control variable (*EGT*) of an isolated intersection is determined on the basis of the state variables considering the traffic condition at the intersection alone, whereas the *EGT* of coordinated sequential intersections is determined on the basis of the traffic conditions of all approaches along the arterial.

An experimental example with three consecutive four-leg intersections (Figure 10) is demonstrated. Assume that the intersections have two lanes in each approach with saturation flow of 1800 pcu/hour/lane. The distance between intersections 1 and 2 is 139 m (five cells). The distance between intersections 2 and 3 is 222 m (eight cells). The 5-minute flow rates in different approaches are shown in Figure 11. Noticeable peak and off-peak traffic patterns are assumed in east and west directions. The offset of progressive coordinated system are 10 and 16 seconds, because the average travel speed between intersections is set as 50 km/hour.

5.2. Model performance

To validate the effectiveness, the control performance of the SGFLC model is compared with the IGFLC, VQ and MQ models. To avoid lengthy discussions, the learning results of SGFLC are not

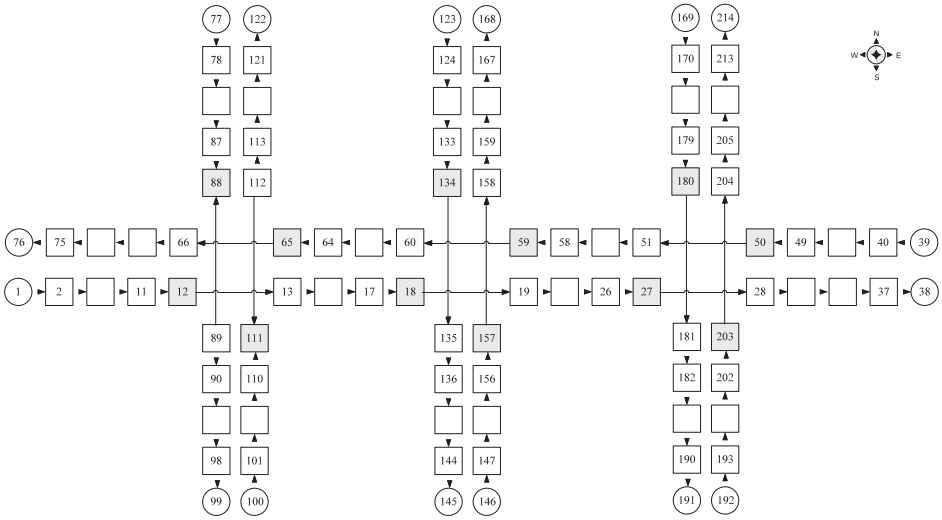

Figure 10. Configuration of the experimental sequential intersections.

DOI: 10.1002/atr

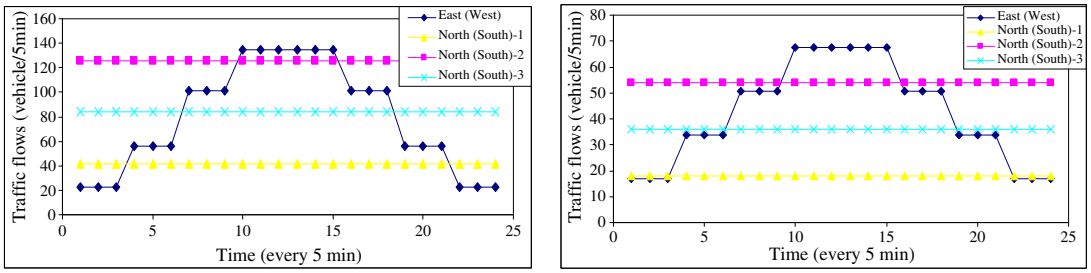

Figure 11. Five-minute (a) car and (b) motorcycle flow rates at the experimental sequential intersections.

reported. The control performances of these control models are reported and compared in Table 6. Obviously, the performances under progressive coordinated system are significantly superior to other systems. The progressive SGFLC model performs best among these four models, followed by the progressive VQ model. The signal control models under alternate coordinated system perform relatively poor. Also notice that all the SGFLC models under various coordinated systems perform better than the IGFLC, VQ and the MQ models. The results show the effectiveness of the proposed SGFLC model in controlling the signal timings of sequential intersections.

5.3. Model application

To further investigate the field applicability of our proposed SGFLC model, a case study on three consecutive intersections along Jin-Ma arterial intersecting with Chang-Mei Road, Chang-Xing Road and Dong-Gu Road in Changhua City, Taiwan has been conducted. Configuration and traffic flow of the three intersections are shown in Figures 12 and 13, respectively. The green times of current timing

Table VI. Comparison of control performance at the experimental sequential intersections.

Signal coordinated system	*TVD* (vehicle-hours)				Rate of Δ*TVD* reduced by SGFLC		
	SGFLC	IGFLC	VQ	MQ	IGFLC (%)	VQ (%)	MQ (%)
Simultaneous	198.44	201.38	201.66	206.24	1.48	1.62	3.93
Progressive	185.21	190.47	189.51	193.76	2.84	2.32	4.62
Alternate	238.98	240.34	241.64	245.21	0.57	1.11	2.61
Independent	211.21	212.67	212.41	216.78	0.69	0.57	2.64

TVD, total vehicle delays; SGFLC, stepwise genetic fuzzy logic control; OS, optimal single; OM, optimal multiple; IGFLC, iterative genetic fuzzy logic control; VQ, vanishing queue; MQ, maximum queue.

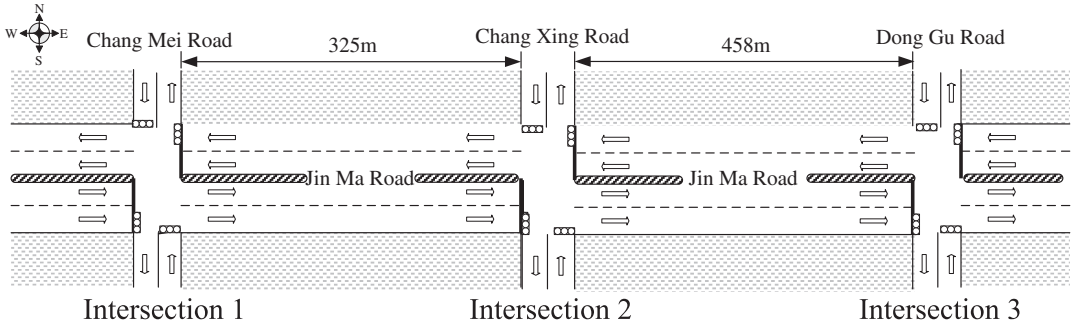

Figure 12. Configuration of the three consecutive intersections along Jin-Ma Road.

DOI: 10.1002/atr

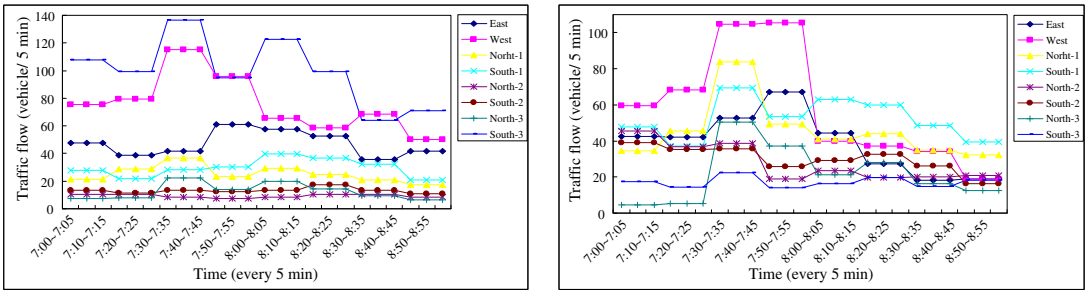

(a) car flow rates (b) motorcycle flow rates

Figure 13. Five-minute (a) car and (b) motorcycle flow rates at the three consecutive intersections along Jin-Ma Road.

plans during the observed period are 40 seconds north–south and 75 seconds west–east at Jin-Ma/Chang-Mei intersection, 50 seconds north–south and 120 seconds west–east at Jin-Ma/Chang-Xing intersection, 50 seconds north–south and 125 seconds west–east at Jin-Ma/Dong-Gu intersection. All-reds and change interval are 6 seconds for all intersections. Currently, there is no signal coordinated control among these three intersections.

The control performances of SGFLC, IGFLC, VQ, MQ and current timing plan are reported in Table 7. Compared with the current timing plan, the progressive SGFLC can curtail the total vehicle delays by the largest amount (18.05%), followed by progressive IGFLC and VQ (15.82% and 15.13%), and with the least reduction (1.08% and 0.32%) by alternate signal system. Also notice that SGFLC consistently outperforms over other single models, no matter which signal system is operated.

6. CONCLUDING REMARKS

This paper summarizes an SGFLC model for signal control for both isolated and sequential intersections with the MCTM traffic behavior modeling. We choose traffic flow and queue length as state variables, extension of green time as the control variable, and total vehicle delays as performance measurement. The validation results of the MCTM demonstrate its capability in replicating the mixed traffic behaviors at the signalized intersection. It is interesting to note that although both average delays of cars and motorcycles would be deteriorated as traffic demand grows, the average delay of cars grow much more rapidly than that of motorcycles, suggesting that the MCTM model can simulate the behaviors of motorcycles that do not follow the lane disciplines and may make lateral drifts breaking into two moving cars in order to keep moving forward.

As to the control performance, under different levels of details of state variable measurement, the proposed SGFLC model can perform better if more detailed levels of state variables are considered. In other words, under mixed traffic conditions, vehicle detectors should be able to accurately detect both traffic flows and queue length of cars and motorcycles. The comparisons among various

Table VII. Comparison of control performance at the three consecutive intersections along Jin-Ma Road.

Signal coordinated system	*TVD* (vehicle-hours)				
	SGFLC	IGFLC	VQ	MQ	Current timing plan
Simultaneous	269.98(11.02%)	274.13(9.65%)	275.88(9.07%)	281.59(7.19%)	—
Progressive	248.65(18.05%)	255.41(15.82%)	257.49(15.13%)	264.64(12.78%)	—
Alternate	296.41(2.31%)	298.45(1.63%)	300.14(1.08%)	302.45(0.32%)	—
Independent	287.54(5.23%)	291.87(3.80%)	296.51(2.27%)	298.12(1.74%)	303.41

TVD, total vehicle delays; SGFLC, stepwise genetic fuzzy logic control; OS, optimal single; OM, optimal multiple; IGFLC, iterative genetic fuzzy logic control; VQ, vanishing queue; MQ, maximum queue.
The percentages in parenthesis represent the rates of *TVD* reduction compared with the current timing plan.

DOI: 10.1002/atr

pre-timed and adaptive signal control models show that the control performance of the SGFLC model is almost the same as the OM model, which is considered as the optimal control under given traffic patterns and is superior to the adaptive models for both cases of an isolated intersection and coordinated intersections. Moreover, the SGFLC model can perform much better than any other models as the traffic flows vary more conspicuously, indicating the robustness of the SGFLC model. It should be mentioned that in comparing to the IGFLC model, our model has better performance, but with much fewer selected rules and shorter evolution time, suggesting the proposed model is more efficient and robust.

The proposed SGFLC model mainly relies on the traffic information including traffic flow and queue length of cars and motorcycles to adaptively control the signal. Through a proper installation of two sets of sensors near the intersections, both traffic flow and queue length can be obtained (e.g., [21]). However, for the intersections with only one set of sensors, queue length can still be estimated on the basis of traffic flow theories, for example, shockwave method proposed by Liu *et al*. [22]. Additionally, the inaccuracy of traffic information detected on urban streets is pretty common. How to conduct an optimal control based on such inaccurate and unreliable vehicle detectors is also an interesting topic that deserves further attempt. Other directions for future study can be identified. Firstly, the proposed stepwise algorithm is to select rules sequentially. However, an early selected rule may not be necessary to be the one of rules in the optimal rule combination. More effective and efficient encoding methods in selecting the logic rules or tuning the membership functions or both deserve to be explored. Secondly, for sequential coordinated intersections, the control performance is measured by *TVD* in this paper. Other performance indices, such as maximum green band, minimum stopping rate, and maximum throughput, deserve to be adopted and examined. Moreover, in this study, only simple two-phase signal control plan is considered. Multi-phase signal control plans with consideration of turning flows at intersections deserve to be developed. Additionally, prior to field installation, the control performances of the trained SGFLC model can be further examined by commonly adopted traffic simulation software packages, such as AIMSUN, VISSIM, PARAMICS, and CORSIM through built-in application programming interfaces, to judge effectiveness of the proposed model. Last, but not least, for simplicity, this study lumps cars and heavy vehicles all together and limits our application to signal coordination along a corridor. To further enhance the comprehensiveness of the proposed model, the mixed traffic with motorcycles, cars, and heavy vehicles (trucks and busses) and the signal control scaled up to the network level should be considered.

7. LIST OF ABBREVIATIONS

7.1. Abbreviations

SCOOT	Split, cycle, and offset optimization technique
SCATS	Sydney coordinated adaptive traffic system
OPAC	Optimization policies for adaptive control
FLC	Fuzzy logic controllers
GFLC	Genetic fuzzy logic controller
IGFLC	Iterative genetic fuzzy logic controller
SGFLC	Stepwise genetic fuzzy logic controller
CTM	Cell transmission model
MCTM	Mixed traffic cell transmission model
GAs	Genetic algorithms
API	Application programming interface
OS	Optimal single timing plan
OM	Optimal multiple timing plan
VQ	Vanishing queue timing plan
MQ	Maximum queue timing plan
AIMSUN, Paramics, VISSIM, CORSIM	Traffic simulation software packages

DOI: 10.1002/atr

ACKNOWLEDGEMENTS

This manuscript is moderately revised from an early work [23] presented at the *International Conference on Advances in Highway Engineering & Transportation Systems 2011*. The authors are indebted to two anonymous reviewers for their insightful comments and constructive suggestions, which help clarify several points made in the original manuscript. The study was partially sponsored by the Taiwan's National Science Council under contract number NSC 100-2221-E-009-121.

REFERENCES

1. Teodorovic D. Fuzzy logic systems for transportation engineering: the state of the art. *Transportation Research Part A-Policy and Practice* 1999; **33**:337–364.
2. Fang FC, Elefteriadou L. Modeling and simulation of vehicle projection arrival–discharge process in adaptive traffic signal controls. *Journal of Advanced Transportation* 2010; **44**:176–192.
3. Papageorgiou M, Papamichail I, Spiliopoulou AD, Lentzakis AF. Real-time merging traffic control with applications to toll plaza and work zone management. *Transportation Research Part C-Emerging Technologies* 2008; **16**:535–553.
4. Wu YZ, Ho CH. The development of Taiwan arterial traffic-adaptive signal control system and its field test: a Taiwan experience. *Journal of Advanced Transportation* 2009; **43**:455–480.
5. Liu HX, Oh JS, Recker W. Adaptive signal control system with online performance measure for a single intersection. *Transportation Research Record* 2002; **1811**:131–138.
6. Jacob C, Abdulhai B. Automated adaptive traffic corridor control using reinforcement learning: approach and case studies. *Transportation Research Record* 2006; **1959**:1–8.
7. Yao R. Sensitivity analysis of optimization models for isolated intersections with short left-turn lanes on approaches. *Journal of Advanced Transportation* 2012. DOI: 10.1002/atr.1185
8. Esawey ME, Sayed T. Unconventional USC intersection corridors: Evaluation of potential implementation in Doha, Qatar. *Journal of Advanced Transportation* 2011; **45**:38–53.
9. Autey J, Sayed T, Esawey ME. Operational performance comparison of four unconventional intersection designs using micro-simulation. *Journal of Advanced Transportation* 2012. DOI: 10.1002/atr.181
10. Liu Y, Chang GL. An arterial signal optimization model for intersections experiencing queue spillback and lane blockage. *Transportation Research Part C-Emerging Technologies* 2011; **19**:130–144.
11. Mirchandani P, Head L. A real-time traffic signal control system: architecture, algorithms, and analysis. *Transportation Research Part C-Emerging Technologies* 2001; **9**:415–432.
12. Daganzo C. The cell transmission model: a dynamic representation of highway traffic consistent with the hydrodynamic theory. *Transportation Research Part B-Methodological* 1994; **28**:269–287.
13. Daganzo C. The cell transmission model, part II: network traffic. *Transportation Research Part B-Methodological* 1995; **29**:79–93.
14. Chiou YC, Hsieh CW. Mixed traffic cell transmission models: development and validation. *Journal of the Chinese Institute of Transportation* 2012; **24**:245–276.
15. Herrera F, Lozano M, Verdegay JL. Tuning fuzzy logic controllers by genetic algorithms. *International Journal of Approximate Reasoning* 1995; **12**:299–315.
16. Michalewicz Z. *Genetic Algorithms + Data Structures = Evolution Programs*. Springer: Berlin, 1992.
17. Logghe S, Immers LH. Multi-class kinematic wave theory of traffic flow. *Transportation Research Part B-Methodological* 2008; **42**:523–541.
18. Chiou YC, Lan LW. Genetic fuzzy logic controller: an iterative evolution algorithm with new encoding method. *Fuzzy Sets and Systems* 2005; **152**:617–635.
19. Lin WH, Lo HK. A robust quasi-dynamic traffic signal control scheme for queue management. *Proceedings of the Thirteenth International Conference of Hong Kong Society for Transportation Studies*, Hong Kong 2008; 563–572.
20. Lan LW, Chiou YC, Lin ZH, Hsu CC. Cellular automaton simulations for mixed traffic with erratic motorcycles' behaviours. *Physica A* 2010; **389**:2077–2089.
21. Sun X, Han LD, Urbanik T. Secondary coordination at closely spaced actuated traffic signals. *Journal of Transportation Engineering* 2011; **137**:751–759.
22. Liu HX, Wu X, Ma W, Hu H. Real-time queue length estimation for congested signalized intersections. *Transportation Research Part C-Emerging Technologies* 2009; **17**:412–427.
23. Chiou YC, Huang YF. Stepwise genetic fuzzy logic signal control under mixed traffic conditions. *Proceedings of the International Conference on Advances in Highway Engineering & Transportation*, Colombo, Sri Lanka, 2011.